Robotica (2017) volume 35, pp. 354–369. © Cambridge University Press 2015
doi:10.1017/S0263574715000545

# Improving transparency of virtual coupling for haptic interaction with human force observer

Myungsin Kim and Dongjun Lee*

*Department of Mechanical and Aerospace Engineering and IAMD, Seoul National University, Seoul, 151-744, Republic of Korea. E-mail: myungsinkim@snu.ac.kr*

(Accepted June 8, 2015. First published online: July 2, 2015)

**SUMMARY**

Relying solely on virtual springs and dampers, the transparency of standard virtual coupling suffers from the device-proxy coordination error when a large interaction force is engaged (e.g., contact tasks) and also from the unmodifiable inertias of the haptic device and the virtual proxy. To overcome these limitations, we propose a novel virtual coupling scheme, which, utilizing passive decomposition and a human force observer, can maintain the device-proxy coordination error even during contact tasks, while also allowing for scaling down (or up) the apparent inertia of the coordinated device-proxy system, thereby, substantially improving transparency of the standard virtual coupling. Experiments are performed to show the performance and passivity of the proposed virtual coupling. Minimum-possible passive inertia scaling is also theoretically established via some positive-real analysis.

KEYWORDS: Human force observer; passive decomposition; passivity; transparency; virtual coupling.

## 1. Introduction

The main aim of haptic systems[1,2] is to allow human users to physically interact with a computer-simulated virtual environment, or virtual objects therein, through a robotic manipulator, which is called the haptic device, serving the roles of both measuring the human motion and generating force feedback for them. To connect the virtual world and the haptic device, many haptic interaction systems adopt the architecture as shown in Fig. 1, where the virtual proxy[3] (or, god-object[4]) is an avatar representing the haptic device in the virtual world, and the virtual coupling defines a rule connecting the virtual proxy and the haptic device.

The virtual proxy is then simulated to follow the pose of the haptic device, while also respecting the physics of the virtual world, in particular, no-penetration constraint,[4–6] energy-consistent penetration,[7] and some desired dynamics of the virtual proxy itself.[8,9] Force feedback to the haptic device is then typically computed as the force output of the spring-damper connection between the virtual proxy and the haptic device. In this paper, following,[1,2] we will collectively call this spring-damper type proxy-device coupling the *standard virtual coupling*.

Although widely used in haptic applications (e.g., voxmap-pointsheel methods,[10,11] haptic rendering with constraints,[3–5] dynamic virtual proxy with inertia,[8,9,12,13] multiuser haptics[14,15]), this standard virtual coupling is lacking to provide *transparency*[*], since: (1) the force feedback via the spring-damper connection necessitates device-proxy coordination error; and (2) the device and the proxy inertias are left unmodified, acting as a "masking" intermediate impedance between the human user and the virtual environment. See Fig. 2. Here, recall that: (1) the spring-damper gains of the standard virtual coupling cannot be made arbitrarily large due to the passivity (i.e., stability)

* Corresponding author. E-mail: djlee@snu.ac.kr

[*] Similar to the case of teleoperation,[16] here, the ideal transparency implies perfect motion coordination between the virtual proxy and the haptic device and zero apparent inertia of the coordinated device-proxy system, so that the human users can interact with the virtual environment with no intermediate impedance in Fig. 1.

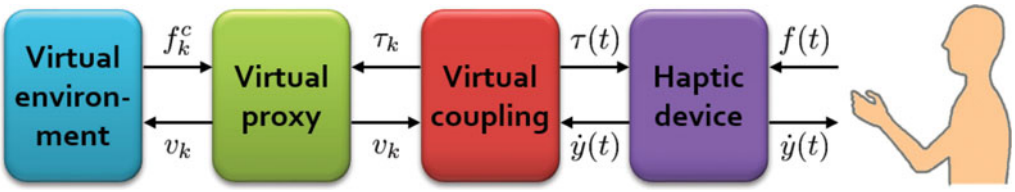


Fig. 1. Block diagram of haptic interaction, where human users interact with virtual environments via the cascade of haptic device, virtual coupling and virtual proxy.

constraint;[17,18] and (2) the device and proxy inertias cannot be made arbitrarily small either, due to the hardware cost and instability triggered by small virtual inertia (e.g., minimum-mass[19]) unless a special passive integrator is used (e.g., ref. [9, 20]).

In this paper, to overcome these limitations of the standard virtual coupling, we propose a novel virtual coupling framework for a multi-DOF haptic device and a dynamic virtual proxy. Our proposed virtual coupling, utilizing passive decomposition[21,22] and a human force observer,[23,24] can maintain the device-proxy coordination even during the contact tasks, while also allowing for scaling down (or up) the apparent inertia of the coordinated device-proxy system, thereby, substantially improving the transparency of the standard virtual coupling. We also experimentally and theoretically show that, as long as the apparent inertia is not scaled down below a certain value (i.e., minimum-possible passive apparent inertia), our proposed virtual coupling can ensure passivity, particularly when used with the passive integration scheme of ref. [9, 20].

More precisely, we employ passive decomposition[21,22] to decompose the nonlinear multi-DOF dynamics of the haptic device and the virtual proxy into that of their coordination error (i.e., shape system) and of their coordinated motion (i.e., locked system). The most remarkable property of this passive decomposition is that it preserves the original robot dynamics structure and their passivity instead of eliminating them (cf. feedback linearization[25]). This then implies that the locked and shape systems both inherit the well-known structure of the nonlinear robot dynamics, thus, we can easily design the inertia scaling control and the device-proxy coordination control for the locked and shape systems, respectively (see Section 3).

These inertia scaling and coordination controls, however, require both the human force $f_1(t) \in \Re^n$ and the virtual proxy force $f_{2,k} \in \Re^n$. Although the virtual force $f_{2,k}$ is available from the simulation, the human force $f_1(t)$ is typically not, as most commercially available haptic devices (e.g., Force Dimension Omega3®, Geomagic Phantom Omni®, Novint Falcon®) are not equipped with force sensors. To circumvent this limitation, we utilize the disturbance observer,[23,24] in particular, the latter for its simplicity and applicability for multi-DOF nonlinear haptic devices.

The inertia scaling and coordination controls, then, utilize force feedforward action to scale up/down, and also cancel out, relevant portions of the human and proxy forces. Such force feedforward action, yet, in general does not enforce passivity, hence possibly resulting in unstable interaction. In this paper, we first experimentally show that if the inertia is not overly scaled down (i.e., $\eta > 0.6$, with $\eta > 1$ and $\eta < 1$ respectively implying inertia scaling-up and scaling-down), our proposed virtual coupling behaves as a passive system. We then provide a theoretical justification on why this is the case, why the inertia scaling-up (i.e., $\eta \geq 1$) is always passive even with force feedforward action, what the minimum-possible passive inertia scaling $\eta_{\min}$ is, and how $\eta_{\min}$ is related to the system dynamics and the human force observer dynamics. This theoretical analysis also sheds light on why our proposed virtual coupling can still ensure passivity without exploiting virtual energy storages, which are typically deemed necessary in telerobotics/haptics[21,26,27] whenever force feedforward action is attempted.

The standard virtual coupling[1,2] is similar to the position-position architecture in telerobotics,[28,29] and it is rather surprising that the virtual coupling in haptics has been mostly restricted to this position-position architecture, which is well known to be inferior in transparency to a four-channel architecture (i.e., the information of both position and force is exchanged).[16] Our proposed virtual coupling is in fact a four-channel extension of the standard virtual coupling, with the abilities of device-proxy coordination and user-specific apparent inertia scaling for general multi-DOF haptic

https://doi.org/10.1017/S0263574715000545 Published online by Cambridge University Press

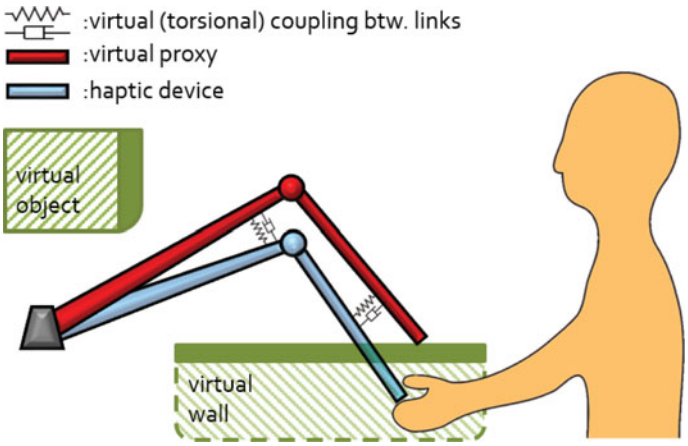


Fig. 2. Degradation of transparency of standard virtual coupling during contact task due to device-proxy position deviation and unscaled inertias of the device and the proxy. Our proposed virtual coupling aims to render the haptic device and the virtual proxy as one single rigid tool with perfect device-proxy coordination and zero apparent device-proxy inertia via inertia scaling.

interaction, while also fully taking into account such issues as the hybrid dynamics/passivity (i.e., continuous-time device and discrete-time proxy) and the lack of force sensors in haptic devices. A similar attempt was undertaken in ref. [24], where a human force observer was also used. However, the result in ref. [24] is limited only to linear/decoupled dynamics, thus, not applicable to multi-DOF nonlinear haptic devices and virtual proxies. Passivity analysis is also missing in ref. [24]. Our proposed virtual coupling may also be thought of as an extension of ref. [21] from the (continuous-time) telerobotics to the (hybrid-time) haptic interaction, with the necessity of utilizing virtual energy storage elements in ref. [21] now completely removed.

A conference version of this manuscript was presented in ref. [30], yet, the issue of passivity was completely neglected and experimental result was also limited only to a simple two-DOF planar interaction there. In contrast, the current manuscript features a new experimental passivity analysis to show that our proposed virtual coupling is passive when the inertia scaling $\eta$ is not so small, and also a theoretical justification on why this is the case by relating the inertia scaling, the system dynamics, and the human force observer bandwidth. An experimental verification using more realistic three-DOF interaction is also performed here.

The rest of this paper is organized as follows. In Section 2, we review the standard virtual coupling and its limitation. Our proposed virtual coupling based on passive decomposition and a human force observer is then presented in Section 3. Experimental results, along with the experimental and theoretical passivity analysis, are presented in Section 4. Concluding remarks are given in Section 5.

## 2. Standard Virtual Coupling and Its Limitation

The virtual coupling in Fig. 1 defines a rule to coordinate the continuous-time haptic device and the discrete-time virtual proxy. The force feedback to the haptic device is typically generated via a (possibly) unilateral virtual spring-damper connection between the proxy and the device.[1–4] Now, consider the second-order dynamic virtual proxies. Then, following ref. [1, 2], the standard virtual coupling establishes a bilateral virtual spring-damper connection between the device and the proxy.

One variant of such standard virtual couplings, studied in ref. [9], is given by the following coordinating torques for the device $\tau_1(t)$ and for the proxy $\tau_{2,k}$: during the time-interval $t \in [t_k, t_{k+1})$,

$$\tau_1(t) := -b_d \dot{x}_1 - b_{vc}\left(\frac{x_{1,k} - x_{1,k-1}}{T_{k-1}} - \bar{v}_{2,k-1}\right) - k_{vc}(x_{1,k} - x_{2,k}) \tag{1}$$

$$\tau_{2,k} := -b_v \bar{v}_{2,k} - b_{vc}\left(\bar{v}_{2,k} - \frac{x_{1,k} - x_{1,k-1}}{T_{k-1}}\right) - k_{vc}(\bar{x}_{2,k} - x_{1,k}) \tag{2}$$

https://doi.org/10.1017/S0263574715000545 Published online by Cambridge University Press

where $T_{k-1} = t_k - t_{k-1} > 0$, $x_1(t) \in \Re^n$ is the configuration of the haptic device with $x_{1,k} \in \Re^n$ being its sampling at $t = t_k$, $x_{2,k}, v_{2,k} \in \Re^n$ are the configuration and the velocity of the virtual proxy at $t = t_k$, $b_d, b_v > 0$ are the minimum device viscous damping and that of the virtual proxy, and $b_{vc}, k_{vc} > 0$ are the damping and spring gains of the virtual coupling. Here, we adopt $\bar{x}_{2,k} := (x_{2,k+1} + x_{2,k})/2$ and $\bar{v}_{2,k} := (v_{2,k+1} + v_{2,k})/2$, following the passive integration scheme of ref. [9, 20] to enhance discrete-time passivity of the virtual proxy simulation, where $x_{2,k+1}$ and $v_{2,k+1}$ are the outputs of the virtual world simulation of the time-interval $T_k$.

Hybrid-time passivity analysis (i.e., continuous-time device and discrete-time proxy) was conducted in ref. [9], and the following passivity condition was obtained for the standard virtual coupling (1)–(2):

$$\begin{aligned} b_d &\geq b_{vc}\left(1 + \frac{T_k}{T_{k-1}}\right) + k_{vc}T_k \\ b_v &\geq \frac{b_{vc}}{2}\left(\frac{T_k}{T_{k-1}} - 1\right) + \frac{k_{vc}T_k}{2} \end{aligned} \tag{3}$$

which shows that (1) the virtual damper and spring, $b_{vc}, k_{vc}$, can generate energy, with $b_{vc}$ acting on the delayed terms $\bar{v}_{2,k-1}, (x_{1,k} - x_{1,k-1})/T_{k-1}$ in (1) and $k_{vc}$ acting on $x_{2,k}$ in (1) instead of $\bar{x}_{2,k}$; and (2) this energy generation should be absorbed by the dampers, $b_d$ and $b_v$. Here, the damper $b_v$ dissipates energy even though it is a virtual damper, as it acts on $\bar{v}_2$.[20]

This passivity condition (3) is in fact similar to that of ref. [17, 19], which, however, lacks the second condition of (3), since the condition of ref. [17, 19] is derived for the virtual wall or with the (impossible) assumption that the virtual world simulation is passive even if it is explicit. Anyhow, the condition (3) and that in ref. [17, 19] all indicate that we cannot increase the spring-damper gains $k_{vc}, b_{vc}$ indefinitely for the standard virtual coupling, since the device's intrinsic damping $b_d$ is bounded and not controllable.

Now, suppose that a human user makes a contact with the virtual environment. Then, some device-proxy coordination error is inevitable, as the force feedback is generated by the virtual spring and damper $k_{vc}, b_{vc}$ as illustrated in Fig. 2. This coordination error then degrades the transparency of the haptic interaction (e.g., confused perception of the boundaries/positions of virtual objects). However, as suggested by the above discussion on the passivity condition (3), we cannot indefinitely increase $k_{vc}$ to suppress this proxy-device deviation. This then means that, to cope with this problem, we would need to use some feedforward action of the human and proxy forces. How to design such feedforward action is not so obvious for multi-DOF nonlinear haptic device and virtual proxy. In Section 3, we will utilize passive decomposition[21,22] to do so, while also utilizing disturbance observer[23,24] to estimate human interaction force.

## 3. Transparent Virtual Coupling Design with Human Force Observer

For real-world-like complex interaction in the virtual environment, the haptic device and the virtual proxy need to possess multi-DOF motion capability. Also, although our approach proposed here is also applicable to other kinds of device-proxy pair (e.g., with redundancy[31]), for simplicity, here, we confine our attention to the case where the haptic device and the virtual proxy are kinematically-similar[21] and their dynamics are given (or simulated) by standard multi-DOF nonlinear robot dynamics.[32]

The virtual proxy may then be thought of as a discrete-time integration mapping $\mathcal{M}$:

$$\mathcal{M}(x_{2,k}, v_{2,k}, \tau_{2,k}, f_{2,k}) \rightarrow (x_{2,k+1}, v_{2,k+1}) \tag{4}$$

where $\tau_{2,k} \in \Re^n$ is the virtual coupling torque and $f_{2,k} \in \Re^n$ is the virtual interaction force. Among many possible integration methods (e.g., backward Euler[19]), in this paper, we adopt the scheme proposed in ref. [9, 20], as it can discrete-time-passively simulate nonlinear robot dynamics. As shown in ref. [33], this simulation passivity then enables us to employ arbitrarily small inertia of the virtual proxy, which is a very desirable property for enhancing transparency. Of course, other

https://doi.org/10.1017/S0263574715000545 Published online by Cambridge University Press

integration schemes can also be used with our proposed virtual coupling. The passivity analysis in Section 4 might not hold for them though, as it relies upon the passivity of the virtual proxy simulation.

Now, we want to design some suitable human/interaction-force feedforward action for the standard virtual coupling (1)–(2) to improve its transparency. For this, here, we utilize passive decomposition[21,22] and a human force observer.[23,24] Let us start with briefly reviewing passive decomposition in the continuous-time domain, which will then be applied to the continuous-time haptic device and the discrete-time virtual proxy. Following ref. [21], consider the dynamics of two $n$-DOF robots:

$$M_1(x_1)\ddot{x}_1 + C_1(x_1, \dot{x}_1)\dot{x}_1 = \tau_1 + f_1 \tag{5}$$

$$M_2(x_2)\ddot{x}_2 + C_2(x_2, \dot{x}_2)\dot{x}_2 = \tau_2 + f_2 \tag{6}$$

where the $x_i, \tau_i, f_i \in \Re^n$ are the configuration, the control torque (i.e., virtual coupling torque) and the external force (i.e., human force and virtual interaction force); and $M_i, C_i \in \Re^{n\times n}$ are the inertia and Coriolis matrices with positive-definite $M_i$ and skew-symmetric $\dot{M}_i - 2C_i$. Here, we assume that the gravity has been locally canceled out or incorporated into the terms $f_1, f_2$.

Passive decomposition[21,22] is then given by the following (non-singular) decomposition matrix:

$$S(x_1, x_2) := \begin{bmatrix} I - \phi(x_1, x_2) & \phi(x_1, x_2) \\ I & -I \end{bmatrix} \in \Re^{2n\times 2n} \tag{7}$$

where $\phi(x_1, x_2) := [M_1(x_1) + M_2(x_2)]^{-1}M_2(x_2)$. Using this, we can then transform the velocity and the control/external forces of (5)–(6) s.t.,

$$\begin{bmatrix} v_L \\ v_E \end{bmatrix} = S(x_1, x_2)\begin{bmatrix} \dot{x}_1 \\ \dot{x}_2 \end{bmatrix}, \qquad \begin{bmatrix} \tau_L + f_L \\ \tau_E + f_E \end{bmatrix} = S^{-T}(x_1, x_2)\begin{bmatrix} \tau_1 + f_1 \\ \tau_2 + f_2 \end{bmatrix} \tag{8}$$

and the dynamics themselves (5)–(6) are also decomposed by

$$M_L(x)\dot{v}_L + C_L(x, \dot{x})v_L + C_{LE}v_E = \tau_L + f_L \tag{9}$$

$$M_E(x)\dot{v}_E + C_E(x, \dot{x})v_E + C_{EL}v_L = \tau_E + f_E \tag{10}$$

where $x := [x_1; x_2] \in \Re^{2n}$ and

$$\begin{bmatrix} M_L & 0 \\ 0 & M_E \end{bmatrix} := S^{-T}\begin{bmatrix} M_1 & 0 \\ 0 & M_2 \end{bmatrix}S^{-1}$$

with $M_L := M_1 + M_2$ and $M_E := \phi^T M_1\phi + [\phi^T - I]M_2[\phi - I]$ being the transformed positive-definite symmetric inertia matrices. The transformed Coriolis matrices are also similarly obtained s.t.,

$$\begin{bmatrix} C_L & C_{LE} \\ C_{EL} & C_E \end{bmatrix} := S^{-T}M\tfrac{d}{dt}(S^{-1}) + S^{-T}CS^{-1} \tag{11}$$

where $M := \mathrm{diag}[M_1, M_2]$, $C := \mathrm{diag}[C_1, C_2]$. From (11), we can also show that $C_{LE} = -C_{EL}^T$, that is, $C_{LE}$ and $C_{EL}$ define conservative (i.e., passive) power shuffling channels between the locked and shape systems.

Here, the dynamics (10) is called the *shape system*, which describes the coordination error $x_E := x_1 - x_2$ with $v_E = \dot{x}_E = \dot{x}_1 - \dot{x}_2$ and with $f_E$ being the "mismatched" portion of the coordination-perturbing human and proxy forces; whereas the dynamics (9) is called the *locked system*, which represents the overall coordinated dynamics of the two robots with $v_L = [M_1 + M_2]^{-1} \cdot [M_1\dot{x}_1 +$

https://doi.org/10.1017/S0263574715000545 Published online by Cambridge University Press

$M_2\dot{x}_2]$ and its inertia and external force respectively given by $M_L = M_1 + M_2$ and $f_L = f_1 + f_2$. For more details on passive decomposition, refer to ref. [21, 22].

Aiming for the ideal transparency (i.e., perfect device-proxy coordination with zero apparent inertia), we design the following controls:

$$\tau_L := C_{LE} v_E + \tfrac{1-\eta}{\eta} f_L, \tag{12}$$

$$\tau_E := C_{EL} v_L - b_{vc} v_E - k_{vc} x_E - f_E, \tag{13}$$

where $\eta > 0$ is the inertia scaling factor to scale down (or up) the apparent inertia of the locked system $M_L$. Applying the controls (12)–(13) to (9)–(10), we can obtain the following closed-loop dynamics:

$$\eta \cdot [M_L(x)\dot{v}_L + C_L(x, \dot{x})v_L] = f_L$$
$$M_E(x)\dot{v}_E + C_E(x, \dot{x})v_E + b_{vc}v_E + k_{vc}x_E = 0$$

where the second line indicates $x_E = x_1 - x_2 \to 0$ exponentially[22,34] even during the contact tasks (i.e., perfect device-proxy coordination), whereas the first line shows that the coordinated device-proxy system will exhibit apparent inertia of $\eta M_L$ (i.e., inertia scaling), with $\eta \to 0$ required for the ideal transparency.

Using (8), we then decode the controls (12)–(13) into $\tau_1$ and $\tau_2$ and apply to the haptic device and the virtual proxy (1)–(2) s.t.,

$$\begin{aligned}\tau_1(t) = &- b_d\dot{x}_1(t) - b_{vc}\left(\tfrac{x_{1,k}-x_{1,k-1}}{T_{k-1}} - \bar{v}_{2,k-1}\right) - k_{vc}(x_{1,k} - x_{2,k}) \\ &+ C_{EL,k}v_{L,k} + \left(I - \phi_k^T\right)C_{LE,k}v_{E,k} + \left(\tfrac{1-\eta}{\eta}I - \tfrac{1}{\eta}\phi_k^T\right)(f_{1,k} + f_{2,k}) + f_{2,k}\end{aligned} \tag{14}$$

$$\begin{aligned}\tau_{2,k} = &- b_v\bar{v}_{2,k} - b_{vc}\left(\bar{v}_{2,k} - \tfrac{x_{1,k}-x_{1,k-1}}{T_{k-1}}\right) - k_{bc}(\bar{x}_{2,k} - x_{1,k}) \\ &- C_{EL,k}v_{L,k} + \phi_k^T C_{LE,k}v_{E,k} + \tfrac{1}{\eta}\phi_k^T(f_{1,k} + f_{2,k}) - f_{2,k}\end{aligned} \tag{15}$$

where $\phi_k$, $C_{EL,k}$, $C_{LE,k}$ are their respective continuous-time variables sampled at $t_k$, and $f_{1,k}$, $f_{2,k}$ are the human force and the proxy force sampled at $t = t_k$. In (14)–(15), similar to (5)–(6), we assume the gravity has been already canceled out locally or embedded in $f_{i,k}$.

Here, note that, in (14)–(15), the portion of standard virtual coupling (1)–(2) is passive under (3). The terms with $C_{LE}$ and $C_{EL}$ turn out not to pose any significant issue either, in terms of passivity due to their skew-symmetric relation $C_{LE} = -C_{EL}^T$. Totally unclear however is whether the remaining terms, which contain the force feedforward actions of the inertia scaling and the cancellation of $f_E$ are passive or not. Their passivity will be experimentally and theoretically established in Section 4.

The proposed virtual coupling (14)–(15) can substantially reduce the device-proxy coordination error even during the contact tasks, while also scaling down (or up, resp.) the apparent inertia of the coordinated proxy-device system with $\eta < 1$ (or $\eta > 1$, resp.), thereby, significantly improving the transparency of the standard virtual coupling. To implement (14)–(15), we need the human force $f_{1,k}$ and the proxy force $f_{2,k}$, where the latter is readily available from the simulation, while the former is not, as most commercial haptic devices do not have force sensors on them. For this, we utilize the disturbance observer proposed in ref. [23, 24], as summarized in Section 3.1, along with a remedy to the issue of device saturation.

### *3.1. Human force observer*

Consider the dynamics of a haptic device (5). The human force may then be considered as a disturbance $d \in \Re^n$ s.t.,

$$d = M(x)\ddot{x} + C(x, \dot{x})\dot{x} - \tau \tag{16}$$

https://doi.org/10.1017/S0263574715000545 Published online by Cambridge University Press

where we omit the subscript for simplicity. Denote the estimate of this disturbance $d$ by $\hat{d} \in \Re^n$, and, following ref. [23], define an auxiliary variable $z \in \Re^n$ s.t.,

$$\hat{d} := z + p$$

where $p \in \Re^n$ is any function satisfying $\dot{p} = LM\ddot{x}$. As suggested in ref. [24], here, we choose $p = L(x)M(x)\dot{x} = \alpha\dot{x}$ with $L(x) = \alpha M^{-1}(x) \in \Re^{n\times n}$ and $\alpha > 0$. The estimate $\hat{d}$ is then updated with the following update dynamics of $z$:

$$\dot{z} = -L(x)z + L(x) \cdot [C(x, \dot{x})\dot{x} - \tau - p] \tag{17}$$

Convergence of this human force observer can then be shown as follows. Define the force estimation error $e_d := d - \hat{d}$. We can then obtain the dynamics of $e_d$ s.t.,

$$\begin{aligned} \dot{e}_d &= \dot{d} - (\dot{z} + L(x)M(x)\ddot{x}) = \dot{d} - L(x)[M(x)\ddot{x} + C(x, \dot{x})\dot{x} - \tau - p - z] \\ &= \dot{d} - L(x)[M(x)\ddot{x} + C(x, \dot{x})\dot{x} - \tau - \hat{d}] = \dot{d} - L(x)e_d \end{aligned} \tag{18}$$

where we use the definitions of $d$ in (16) and $\hat{d}$, the update equation (17), and the condition $\dot{p} = LM\ddot{x}$. This then implies that, by choosing $\alpha$ large enough w.r.t. $||\dot{d}||$, there will exist a finite time $t_{\text{ub}} \geq 0$ s.t., $||e_d(t)|| \approx 0$ for all $t \geq t_{\text{ub}}$, since (1) with $L(x) = \alpha M^{-1}(x)$, the error dynamics of $e_d$ (18) is ultimately bounded; and (2) in typical haptic interaction, a human command (e.g., $||\dot{d}||$) does not change so quickly (e.g., see Fig. 7), thus, we can indeed set $\alpha$ (or observer bandwidth $w_f$) large enough to make the ultimate bound of $e_d$ small enough. See Section 4.

Although we found this human force observer (17) adequately functioning during our experiments, we also found that it exhibited "lurking" and "wind-up" phenomena, when the device control $\tau_1(t)$ becomes saturated. To better see this, consider a static contact. To make exposition simpler, consider also only one axis of the haptic device. Then, the real device control $\tau$ will be $\tau = \tau_m$ if $\tau_c \geq \tau_m$; or $\tau = \tau_c$ if $\tau_c \leq \tau_m$, where $\tau_c$ is the intended torque command and $\tau_m$ the maximum possible (saturated) control torque.

Now, suppose that $\tau$ is saturated by $\tau_m$, yet, this is not properly reflected in the force estimation (17). Then, in steady-state, the estimated force will be $\hat{d} = -\tau_c$ (from (17)), yet, the real force is $d = -\tau_m$ (from (16)). Combining these two equations, we can then obtain

$$\hat{d} = d - (\tau_c - \tau_m)$$

showing that the observer $\hat{d}$ will over-estimate the real human force $d$ by the magnitude of $\tau_c - \tau_m \geq 0$, increasing the feedforward terms in the virtual coupling (14)–(15). Here, note that, in static contact, the signs of $d$ and $\tau$ are opposite.

Since the feedforward terms in (14)–(15) attempt perfect coordination and the device torque $\tau$ is already saturated, the haptic device will stay where it is, yet, the virtual proxy will start moving toward the haptic device. This then means that, during the static contact, the virtual proxy will "lurk" by itself, e.g., to the boundary of the virtual wall in Fig. 2. During this process, the estimated force $\hat{d}$ may also accumulate to a large value (via (17)). Then, when the human user tries to pull the haptic device out from the virtual wall, $\hat{d}$ may still be large, generating abnormally large pushing force from the virtual wall.

To prevent these "lurking" and "wind-up" phenomena, we choose to use $\tau_m$ instead of $\tau_c$ in the force observer (17) whenever $\tau_c \geq \tau_m$. This simple strategy turns out to be fairly effective in practice. This saturation problem was also considered in ref. [24] by projecting $\hat{d}$ directly below $\tau_m$ (instead of $\tau$).

### *3.2. Robustness against inertial parameter uncertainty*

Our proposed virtual coupling (14)–(15) requires inertial parameters of the haptic device, which are difficult to obtain exactly in practice. Our virtual coupling (14)–(15), however, turns out to be robust against this inertial uncertainty, as to be shown theoretically below and also experimentally in Section 4 (e.g., see Fig. 4). This robustness is not so obvious from (14)–(15) though, since many terms there,

https://doi.org/10.1017/S0263574715000545 Published online by Cambridge University Press

particularly those related to the force feedforward actions, will be affected by the uncertainty (e.g., $\phi$, $v_L$, $C_{LE}$, $C_{EL}$), hence becoming potentially harmful rather than helpful.

Now, to analyze the robustness of our virtual coupling against the inertial uncertainty, let us start with the decomposed dynamics (9)–(10). Then, we can obtain the following perturbed locked-shape dynamics:

$$\begin{pmatrix} M_L\dot{v}_L + C_L v_L + C_{LE} v_E \\ M_E\dot{v}_E + C_E v_E + C_{EL} v_L \end{pmatrix} = S^{-T}\hat{S}^T \begin{pmatrix} \tau_L \\ \tau_E \end{pmatrix} + \begin{pmatrix} f_L \\ f_E \end{pmatrix} \tag{19}$$

where $\hat{S}$ and $S^{-T}\hat{S}^T$ are given by

$$\hat{S} := \begin{bmatrix} I - \hat{\phi} & \hat{\phi} \\ I & -I \end{bmatrix}, \quad S^{-T}\hat{S}^T = \begin{bmatrix} I & 0 \\ \phi^T - \hat{\phi}^T & I \end{bmatrix}$$

with $\hat{\star}$ representing the term $\star$ under the uncertainty.

From (19) with (12), we can then see that the inertia scaling control will almost retain its effectiveness even under the inertial uncertainty, since the perturbed locked system dynamics in this case is given by

$$\eta \cdot [M_L\dot{v}_L + C_L v_L + (C_{LE} - \hat{C}_{EL})v_E] = f_L \tag{20}$$

where $f_L = f_1 + f_2$ does not suffer from the inertial uncertainty and $||v_E||$ is typically not so large during the experiments (see Fig. 4). From (19) with (13), we can also obtain the perturbed shape system dynamics s.t.,

$$M_E\dot{v}_E + C_E v_E + b_{vc} v_E + k_{vc} x_E + (C_{EL} - \hat{C}_{EL})v_L = \tfrac{1}{\eta}\tilde{\phi}^T f_L \tag{21}$$

where $\tilde{\phi} := \phi - \hat{\phi}$ and we use $\frac{1-\eta}{\eta}\tilde{\phi} f_L - \hat{f}_E + f_E = \frac{1}{\eta}\tilde{\phi}^T f_L$ with $\hat{f}_E = \hat{\phi}^T(f_1 + f_2) - f_2$. However, during contact tasks, we have $\dot{x}_i \to 0$, which, from the above locked system dynamics (20), means that $f_L \to 0$. This then in turn implies from (21) that, with $\hat{f}_E \to f_E$ and $(\dot{v}_E, v_E) \to 0$, perfect device-proxy coordination will be guaranteed (i.e., $x_E \to 0$) even under the uncertainty.

Note from (1)–(2) and (14)–(15) that our proposed virtual coupling can be implemented on top of the (already-coded) standard virtual coupling. Also, as can be seen from (14)–(15), the structure of our proposed virtual coupling is rather straightforward and amenable to real-time implementation, only with the first-order human force observer (17) and the static feedforward/feedback control actions. The implementation of our virtual coupling (14)–(15) will yet become involved if the haptic device has large-DOF, since, in this case, some terms in our virtual coupling (14)–(15) (e.g., $\phi_k = [M_{1,k} + M_{2,k}]^{-1} M_{2,k}$) and also in the human force observer (17) (e.g., $L(x) = M^{-1}(x)$) can become high-dimensional/complicated. Recall though that: (1) our proposed virtual coupling possesses the robustness against this inertial uncertainty as shown above; and also (2) typical (or commercial) haptic devices have rather limited-DOF with their inertial parameters also often known. How to extend our proposed virtual coupling for haptic devices with large-DOF, possibly utilizing some iterative algorithms to handle the aforementioned high-dimensional and complex terms, is a topic for future research.

## 4. Experimental Results and Passivity Analysis

Here, we first perform experimental validation of our transparent virtual coupling developed so far (Section 4.1). We then present theoretical passivity analysis for the experimental result of Section 4.1, particularly why there exists the minimum-possible passive inertia scaling $\eta_{\min}$ and how this $\eta_{\min}$ is related to the system dynamics and the human force observer dynamics.

https://doi.org/10.1017/S0263574715000545 Published online by Cambridge University Press

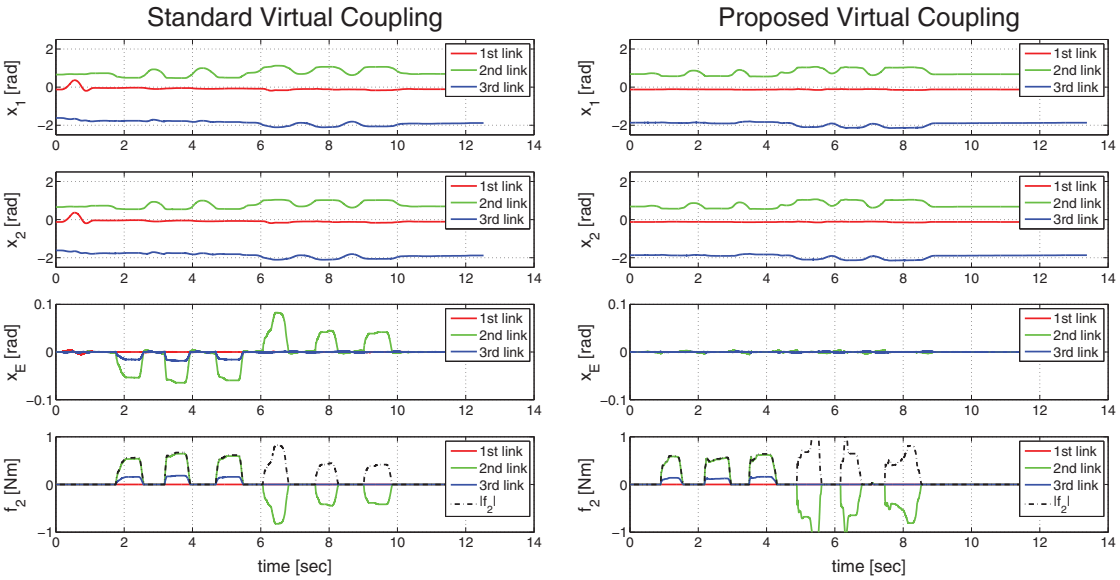


(a) Standard virtual coupling (1)-(2)

(b) Proposed virtual coupling (14)-(15)

Fig. 3. Comparison of the standard virtual coupling (1)–(2) with the proposed virtual coupling (14)–(15) during 3-DOF haptic interaction with intermittent contacts, the first three on the middle of the proximal link and the last three on the end-effector. Notice our proposed virtual coupling maintains the device-proxy coordination even during the contacts, whereas the standard virtual coupling does not.

### *4.1. Experimental verification*

We implement our proposed virtual coupling (14)–(15) on the actuated three-DOF of a Phantom Omni®, whose inertial parameters are obtained via least-square identification. We also render a three-DOF virtual proxy, kinematically similar to the haptic device. We allow this virtual proxy to make multi-point/intra-link contacts, that is, on the middle of its proximal link and also at the end-effector of the distal link. See Fig. 2. Both of these intra-link and end-effector contacts are rendered as pure stiffness contacts with no damping dissipation, with their respective stiffness set by $K_{\text{proximal}} = 20$[Nm/rad] and $K_{\text{end-tip}} = 600$[N/m]. The integration method of ref. [9, 20] is utilized to simulate the multi-DOF nonlinear dynamics of the virtual proxy and the linear elastic dynamics of the virtual objects. Due to its enforcing discrete-time passivity, this integration method[9,20] enables us to choose a very small inertia of the virtual proxy (and also very large stiffness if the contact is sustained). We choose the inertia of the virtual proxy to be of the order of around $10^{-4}$ w.r.t. the inertia of the haptic device. The device servo-rate and the virtual world simulation rate are both $T_k = 1$[ms].

For the standard virtual coupling (1)–(2), we set its gains to be $k_{vc} = 10$[Nm/rad] and $b_{vc} = 0.001$[Nm s/rad]. To choose these gains, we increase $k_{vc}$ until the device starts to vibrate, which corresponds to the first condition of (3). We also set $b_v = 0.012$[Nm s/rad] to be around twice larger than that as required by the second condition of (3) to suppress vibration during the contact on–off switching with the virtual objects. How to passively simulate such a contact switching is beyond the scope of this paper (i.e., virtual coupling itself, not virtual world simulation) and is a topic for future research, for which we believe the passive integration scheme of ref. [9, 20] would be useful, as it can enforce passivity of the *sustained contact* with any arbitrary viscoelastic virtual objects. We also empirically optimize the human force observer gain to be $\alpha = 0.035$ with the performance-passivity/robustness trade-off (i.e., set $\alpha$ as high as possible for the performance (cf. (18)), yet, not so high to passively attain the desired scaled-down inertia (cf. (25)) and also robustness against noise, etc.) and found its bandwidth to be $w_f \approx 200$[rad/s].

In the first experiment, we compare the performance of the standard virtual coupling (1)–(2) with that of our proposed virtual coupling (14)–(15). A human user makes three successive contacts on the proximal link, and then another three contacts at the end-effector of the three-DOF virtual proxy by manipulating the three-DOF haptic device. The user tries his/her best to make the haptic interaction as similar as possible between the two virtual coupling schemes. The results are presented

https://doi.org/10.1017/S0263574715000545 Published online by Cambridge University Press

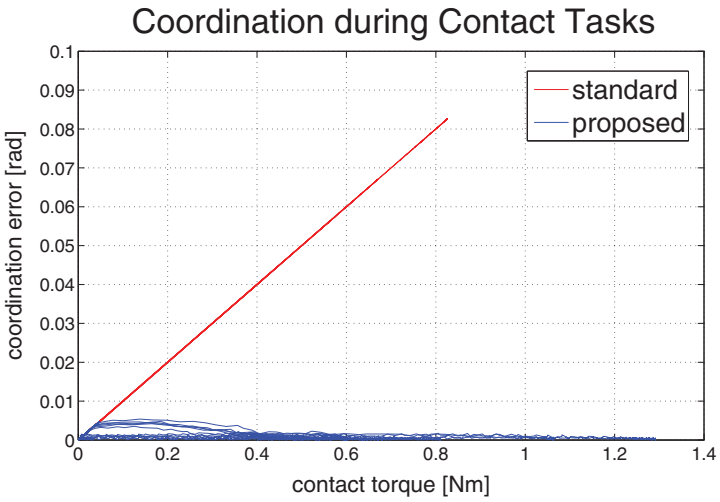


Fig. 4. Device-proxy coordination performance of the standard virtual coupling and the proposed virtual coupling. Our proposed virtual coupling can maintain the coordination regardless of contact force, whereas coordination error of the standard virtual coupling is proportional to contact force.

in Fig. 3, where we can see that our proposed virtual coupling (14)–(15) can maintain very good proxy-device coordination even during the contacts, while the standard virtual coupling (1)–(2) exhibits substantial device-proxy coordination error during the contacts. This significantly enhanced coordination performance of our proposed virtual coupling can even be better seen from Fig. 4, where, for the standard virtual coupling, the coordination error is proportional to the contact force, while, for our proposed virtual coupling, the coordination error is bounded and remains small regardless of the magnitude of the contact force.

The second experiment is performed to show the efficacy of our inertia scaling control with $\eta = \{0.6, 1, 5\}$. For this, the human user manipulates the three-DOF haptic system to incur a temporally/spatially-similar free motion of the virtual proxy with the different inertia scaling factors. The results are shown in Fig. 5, where we can see that the human force, required to produce this spatially/temporally similar free motion and estimated by our human force observer, gets smaller with $\eta = 0.6$ (i.e., apparent inertia scaled-down) and larger with $\eta = 5$ (i.e., apparent inertia scaled-up) as compared to the case of $\eta = 1$ (i.e., no apparent inertia scaling). The results in Fig. 5 together with that in Fig. 3 then clearly indicate that, with $\eta = 0.6$, our proposed virtual coupling (14)–(15) substantially improves the transparency of the standard virtual coupling (1)–(2), with much less intermediate impedance between the haptic device and the virtual proxy in Fig. 1.

Finally, the third experiment is conducted to experimentally show that our proposed virtual coupling (14)–(15), even with the force feedforward action, still enforces passivity when $\eta$ is not so small. For this, a human user performs a succession of free motion, contact with the wall and circle-drawing on the contact surface. The user carries out 10 trials of this composite scenario with $\eta \in \{0.6, 1, 3, 5\}$ and also with the standard virtual coupling. The user also controls the operation time to be similar among these trials so that we can compare their time-averaged passivity property as shown in Fig. 6. For this, since we do not have a human force sensor (although we do have a human force observer), we compute **controller passivity**,[21] i.e.,

$$E_{c,NT} := \sum_{k=0}^{N} \left[\tau_{1,k} \cdot (x_{1,k+1} - x_{1,k}) + \tau_{2,k} \cdot (x_{2,k+1} - x_{2,k})\right] \leq 0, \quad \forall N \geq 0$$

where $T = 1$[ms] is the sampling rate, and $\tau_{1,k}$ is the zero-order-hold value of the haptic device control $\tau_1(t)$ at the time-instance $kT$. As shown in,[21] this controller passivity implies the (closed-loop) passivity of our proposed virtual coupling. We can then see from Fig. 6 that: (1) standard virtual coupling under the passivity condition (3) is indeed passive; (2) our proposed virtual coupling is less passive than the standard virtual coupling if $\eta < 1$ and more passive if $\eta > 1$; and (3) our proposed

https://doi.org/10.1017/S0263574715000545 Published online by Cambridge University Press

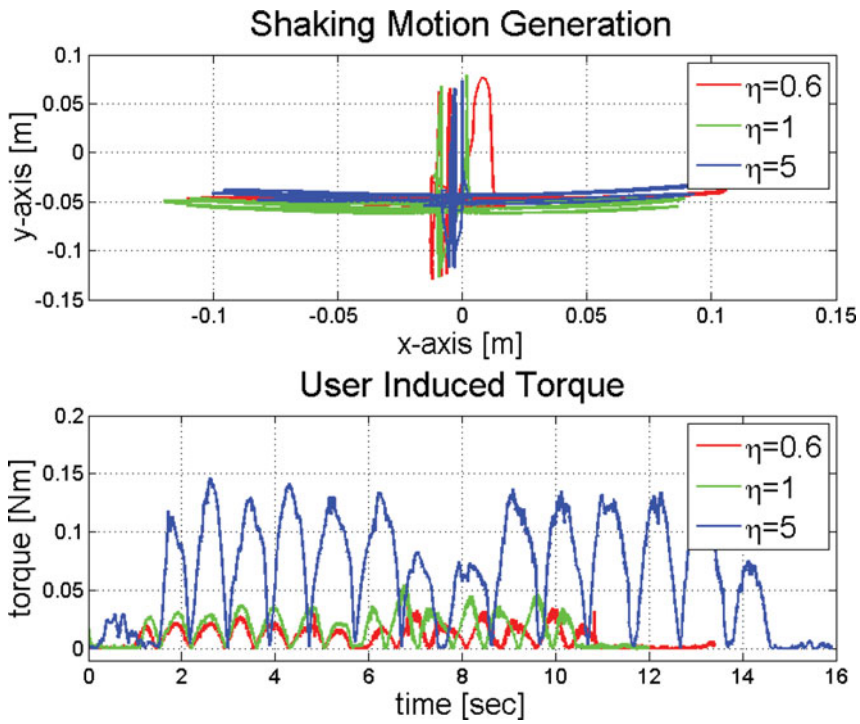


Fig. 5. Comparison of human forcing to generate spatially/temporally similar free motion with three different inertia scaling factors. Notice that the human force gets smaller with $\eta = 0.6$ (i.e., inertia scaled-down) and larger with $\eta = 5$ (i.e., inertia scaled-up) as compared to $\eta = 1$ (i.e., no inertia scaling).

virtual coupling is passive even with the force feedforward action, if $\eta$ is not so small (i.e, becomes not passive with $\eta \leq 0.5$: not shown here).

In Section 4.2, we elucidate why the inertia scaling $\eta$ affects the passivity of our proposed virtual coupling in this way, i.e., why a smaller inertia scaling $\eta < 1$ reduces the "margin" of passivity (i.e., margin from the zero-line in Fig. 6) and why the scaled-up inertia (i.e., $\eta > 1$) still enforces passivity even if the human/virtual force feedforward actions are present in (14)–(15) with their effect getting more intensified as $\eta$ increases from $\eta = 1$ to $\eta \to \infty$. This theoretical passivity analysis and the experimental observations in Fig. 6 were missing in ref. [30] and are presented here for the first time.

### *4.2. Passivity analysis with inertia scaling $\eta$*

The unabridged passivity analysis of our proposed virtual coupling with the multi-DOF haptic device and the virtual proxy is excessively difficult, or more likely, impossible, since it is a nonlinear, hybrid, and multi-input-multi-output system with arbitrary forcing ($f_1$, $f_2$) and such complex issues as Coulomb friction, sensing uncertainty/quantization, etc. To make our analysis feasible while still retaining essential relation between the inertia scaling $\eta$ and passivity, we make the following simplifying assumptions motivated by observation of the system behavior during our experimental studies.

We first assume that the dominant effect of the inertia scaling on passivity can be captured by the continuous-time dynamics, i.e., similar to (19), we utilize the following dynamics for our analysis here:

$$\begin{pmatrix} M_L \dot{v}_L + C_L v_L + C_{LE} v_E \\ M_E \dot{v}_E + C_E v_E + C_{EL} v_L \end{pmatrix} = \begin{pmatrix} \tau_L + f_L \\ (\phi^T - \hat{\phi}^T)\tau_L + \tau_E + f_E \end{pmatrix} \tag{22}$$

with $\tau_L = \hat{C}_{LE} v_E + \frac{1-\eta}{\eta} \hat{f}_L = \hat{C}_{LE} v_E + \frac{1-\eta}{\eta}(\hat{f}_1 + \hat{f}_2)$ and $\tau_E = \hat{C}_{EL} \hat{v}_L - b_{vc} v_E - k_{vc} x_E - \hat{f}_E$, where $\hat{\star}$ is $\star$ with the inertial uncertainty or the force observer inaccuracy. This simplification, we believe, is adequate, since, here, we aim to analyze passivity as related to $\eta$, not related to the sampling or other discrete-time phenomena.

https://doi.org/10.1017/S0263574715000545 Published online by Cambridge University Press

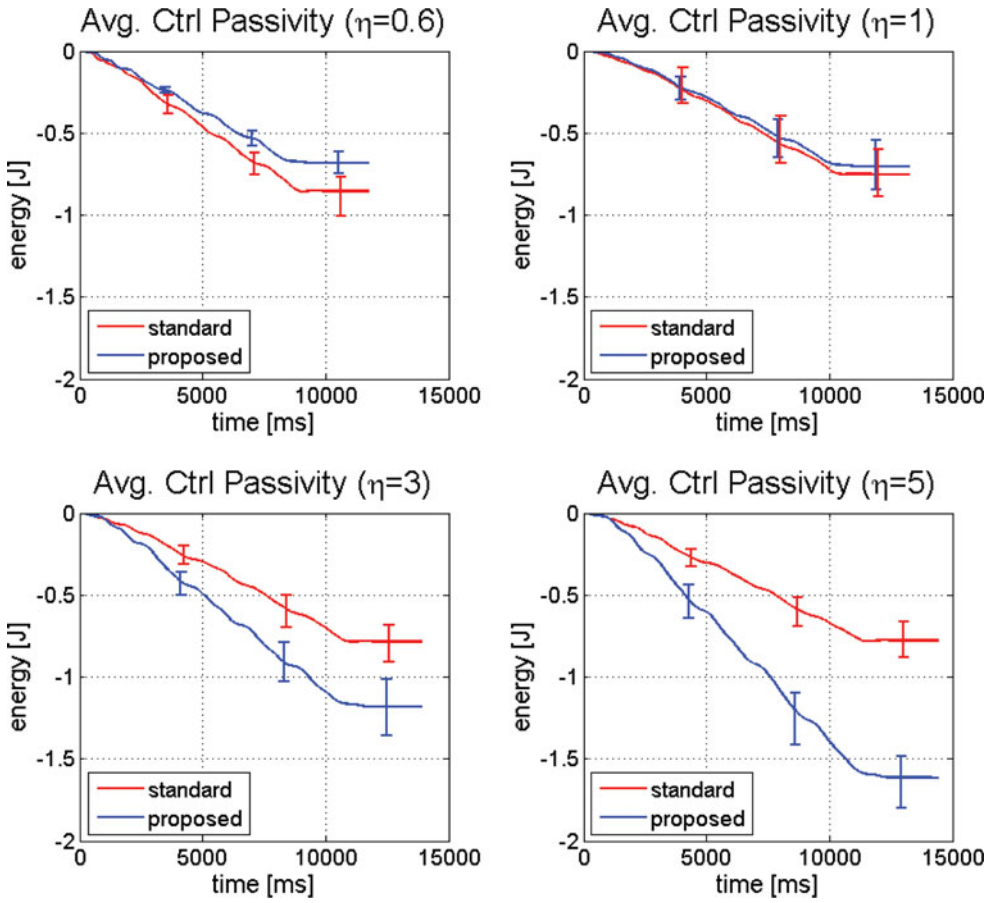


Fig. 6. Controller passivity $E_c$ of the proposed virtual coupling and the standard virtual coupling (averaged for 10 trials with minimum/maximum indicated too). Notice that inertia scaling down (i.e., $\eta < 1$) reduces "margin" of passivity, whereas inertia scaling up (i.e., $\eta > 1$) increases this margin, implying that our proposed virtual coupling is passive if $\eta$ is not so small. See Section 4.2 for theoretical analysis.

We further make the following assumptions, which are also motivated by our observation of the experimental results in Figs. 3–6:

- The shape system dynamics of $v_E$ is not dominant on the relation between passivity and $\eta$, as we observed that $x_E$ remains bounded (see Fig. 4) and behaves similarly during all the experiments in Fig. 6, implying that the most prevailing factor on passivity in Fig. 6 is $\eta$ (i.e., locked system dynamics).
- The effects of $C_L, C_E, C_{LE}, C_{EL}$ are all negligible, as the operations in Fig. 6 are not so fast.
- $\phi \approx \hat{\phi}$, since, in $\phi = [M_1 + M_2]^{-1} M_2$, the device inertia $M_1$ is the only uncertain term, and the virtual proxy inertia $M_2$ is set much smaller than $M_1$ as stated in the beginning of Section 4.
- $\hat{F}_L(s) \approx \frac{w_f}{s+w_f} F_L(s)$, where $s \in \mathbb{C}$ is the Laplace variable and $w_f \geq 0$ is the cut-off frequency of the human force observer (18). We make this assumption here even though $\hat{f}_L = \hat{f}_1 + \hat{f}_2$, as we observed from our experiments that non-passive oscillation occurs typically during the free-motion (i.e., with $f_2 \approx 0$), not during the contacts, for which the system behavior becomes much less oscillatory (i.e., likely more passive).

With these simplifying assumptions, the closed-loop dynamics (22) is reduced to

$$m_L \ddot{x}_L + b_L \dot{x}_L = \tfrac{1-\eta}{\eta} \hat{f}_L + f_L \tag{23}$$

where, for simplicity, we also assume that the locked dynamics in (22) is a scalar system with $m_L := m_1 + m_2 > 0$, $x_L := (m_1 x_1 + m_2 x_2)/m_L \in \Re$ with $v_L = \dot{x}_L$, and $b_L > 0$ is the damping stemming

https://doi.org/10.1017/S0263574715000545 Published online by Cambridge University Press

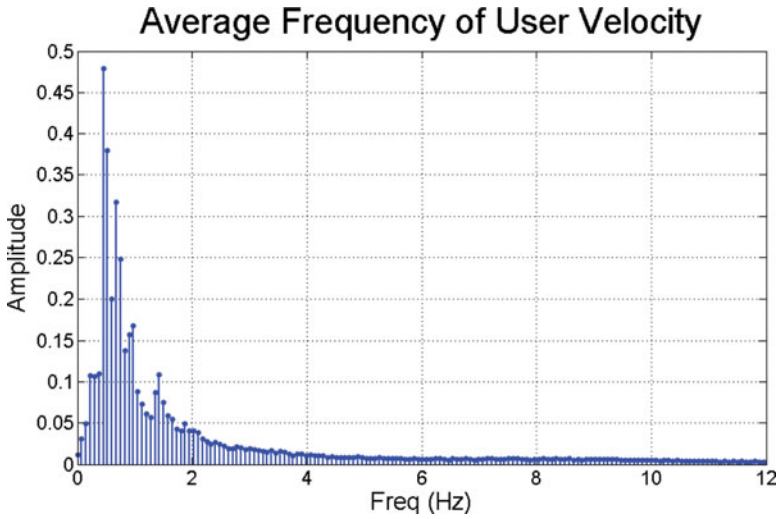


Fig. 7. Frequency content of human motion during the experiments in Fig. 6 averaged over time. Note that the frequency content is mostly limited below 5 Hz.

from $b_d$ and $b_v$ of (14), (15). Then, applying the Laplace transform, we have

$$V_L(s) = \frac{1}{m_L s + b_L} \cdot \left(1 + \frac{1-\eta}{\eta} \frac{w_f}{s + w_f}\right) F_L(s) =: H_L(s) F_L(s) \tag{24}$$

suggesting that passivity can be argued if and only if the transfer function $H_L(s)$ is positive-real (PR), i.e., its Nyquist plot lies in the RHP (right-half plane) in the complex domain.[25]

Now, to see when the transfer function $H_L(s)$ is PR, we compute $H_L(jw)$ and check when its real-component is non-negative, i.e., $\mathrm{Re}[H_L(jw)] \geq 0 \ \forall w \in [0, +\infty)$, where $j := \sqrt{-1}$. It is then easy to show that this is equivalent to

$$R_L(w) := w_f^2 + \frac{\eta(w_c + w_f) - w_f}{w_c} w^2 \geq 0, \quad \forall w \in [0, +\infty)$$

where $w_c := \frac{b_L}{m_L}$ and $w_f$ are the bandwidths of the open-loop locked system dynamics (23) and the human force observer (18). We can then show that $H_L(s)$ is PR iff

$$\eta \geq \frac{w_f}{w_c + w_f} \tag{25}$$

from which we can extract the following observations in concert with the experimental results in Figs. 3–6:

- Even though the force feedforward actions are utilized, the apparent inertia scaling-up (i.e., $\eta \geq 1$) is always passive, whereas passively scaling-down the apparent inertia (i.e., $\eta < 1$) is lower-bounded by a certain minimum-possible passive inertia scaling $\eta_{\min} := w_f/(w_c + w_f)$ (see Fig. 6).
- Larger damping $b_L$ or smaller inertia $m_L$ of the open-loop locked system (23) will allow for further reduction of the minimum-possible passive inertia scaling $\eta_{\min}$, as, in this case, we have more "passifying" damping effect and/or need less inertia scaling-down control action with $m_L$ already small.
- A slower human force observer is more favorable to passively "include" smaller inertia scaling $\eta$, but not to necessarily "achieve" this intended $\eta$ (i.e., passivity is enforced, yet, the inertia scaling $\eta$ itself may be incompetent and not fully effective).

For our experimental setup, we have $w_f \approx 200$[rad/s] as stated in the beginning of Section 4. We also estimate $w_c = b_L/m_L \approx b_d/m_1 \approx 50$[rad/s], since: (1) for Phantom Omni®, we can estimate

https://doi.org/10.1017/S0263574715000545 Published online by Cambridge University Press

$b_d \approx 1.912$[Ns/m] by using the Colgate's passivity condition[17] and also have its apparent inertia to be $m_1 \approx 45$[g] according to the manufacturer's website†; and (2) the inertia and damping of the virtual proxy are set to be much smaller than those of Phantom Omni, thus, their contribution to $m_L, b_L$ is rather negligible.

If we use the condition (25), we can then estimate $\eta_{\min} \approx 0.8$, which is heavier than $\eta = 0.6$ of our experiments in Fig. 6. Among many possible sources of this conservatism (e.g., unmodeled phenomena), a particularly interesting one is that our passivity analysis here is based on the assumption that non-passive behavior can arise for *any* frequency $w \in [0, +\infty)$, yet, in practice, human motions are only of limited bandwidth with perception-action asymmetry.[35] For instance, see Fig. 7 for the (averaged) frequency content of human motions during the experiments of Fig. 6, where the frequency content is limited mostly below 5 Hz. This then means that we need to check the PR condition of $H_L(s)$ *only* for this limited bandwidth, not for all $w \in [0, +\infty)$. This may then allow us to substantially reduce the conservatism of the condition (25). How to estimate the minimum-possible passive apparent inertia, while incorporating human perception-action bandwidths (and other un-modeled phenomena) is a topic for future research. See ref. [36, 37] for some related results along this direction.

Recall that our passivity analysis performed here relies on several assumptions made above. This then means that our analysis is not without restriction and should be applied with caution for cases where those assumptions are not granted, for instance: (1) the sampling rate is slow so that its effect on passivity is non-negligible; (2) the device-proxy coordination is compliant so that the shape system $x_E$ dynamics becomes important; (3) the haptic interaction is so fast that the Coriolis effect becomes prominent; (4) the human force observer is of higher order, or with dc-gain error and delay so that the first-order model above becomes invalid; and (5) virtual proxy inertia $M_2$ cannot be made arbitrarily small or major modes of instability occur during contacts (e.g., not using special passive integrators[9,20]).

It is also worthwhile to mention that our passivity analysis here: (1) can be easily extended to the apparent inertia scaling problem of general human-interactive robots; and (2) explains why it is possible to completely eliminate any virtual energy storage elements in our proposed virtual coupling (under the condition (25)), which are in general deemed necessary in telerobotics/haptics to passively produce any force feedforward actions (e.g., ref. [21, 26]).

## 5. Conclusion and Future Work

In this paper, we propose a novel multi-DOF virtual coupling scheme to substantially improve the transparency of the widely used spring-damper type standard virtual coupling. Our proposed virtual coupling utilizes suitably designed human/proxy-force feedforward action to significantly reduce device-proxy coordination error even during the contact tasks, while also allowing for scaling down (or up) the apparent inertia of the coordinated device-proxy system. Passive decomposition[21,22] is used to design the feedforward action and the disturbance observer[23,24] to estimate human force for haptic devices without on-board force sensors. Experiments are performed to show the performance and passivity of our proposed virtual coupling. A theoretical analysis is also provided to show that our proposed virtual coupling is passive if the inertia scaling $\eta$ is not so small.

Some interesting directions for future research include: (1) extension to incorporate human perception-action characteristics and to other general physical human-robot interaction applications; and (2) inclusion of time-varying or skew-symmetric structures (e.g., ref. [21]) to passively implement inertia scaling even less than $\eta_{\min}$.

## Acknowledgments

This research was supported in part by the Global Frontier R&D Program on ⟨Human-centered Interaction for Coexistence⟩ of the National Research Foundation (NRF) of Korea funded by MEST (NRF-2013M3A6A3079227), the Basic Science Program of the NRF of Korea funded by MEST (NRF-2012R1A2A2A01015797), and the Brain Korea 21 Plus Project.

† http://www.geomagic.com/en/products/phantom-omni/specifications

## References


1. J. E. Colgate, M. C. Stanley and J. M. Brown, "Issues in the haptic display of tool use," *Proceedings of IEEE/RSJ International Conference on Intelligent Robots and Systems*, vol. 3, Pittsburgh, PA, USA (1995) pp. 140–1995.
2. R. J. Adams and B. Hannaford, "Stable haptic interaction with virtual environments," *IEEE Trans. Robot. Autom.* **15**(3), 465–474 (1999).
3. P. Mitra and G. Niemeyer, "Dynamic proxy objects in haptic simulations," *Proceedings of IEEE Conference on Robotics, Automation & Mechatronics*, Barcelona, Spain (2004) pp. 1054–2004.
4. C. B. Zilles and J. K. Salisbury, "A constraint-based god-object method for haptic display," *Proceedings of IEEE/RSJ International Conference on Intelligent Robots & Systems 95. 'Human Robot Interaction and Cooperative Robots'*, vol. 3, Pittsburgh, USA (1995) pp. 146–1995.
5. M. Ortega, S. Redon and S. Coquillart, "A six degree-of-freedom god-object method for haptic display of rigid bodies with surface properties," *IEEE Trans. Vis. Comput. Graph.* **13**(3), 458–469 (2007).
6. G. Yu, D. Wang and Y. Zhang, "Accelerating optimization-based haptic rendering by parallel quadratic programming method," *Proceedings of IEEE/RSJ International Conference on Intelligent Robots & Systems*, Tokyo, Japan (2013) pp. 4499–2013.
7. M. Kolesnikov and M. Zefran, "Energy-based 6-dof penetration depth computation for penalty-based haptic rendering algorithms," *Proceedings of IEEE/RSJ International Conference on Intelligent Robots & Systems*, San Diego, USA (2007) pp. 2120–2007.
8. G. Cirio, M. Marchal, M. A. Otaduy and A. Lécuyer, "Six-dof haptic interaction with fluids, solids, and their transitions," *Proceedings of World Haptics Conference*, IEEE, Daejeon, Korea (2013) pp. 157–162.
9. D. J. Lee, M. Kim and T. Qiu, "Passive haptic rendering and control of lagrangian virtual proxy," *Proceedings of IEEE/RSJ International Conference on Intelligent Robots & Systems*, Algarve, Portugal (2012) pp. 64–2012.
10. M. Renz, C. Preusche, M. Pötke, H.-P. Kriegel and G. Hirzinger, "Stable haptic interaction with virtual environments using an adapted voxmap-pointshell algorithm," *Proceedings of Eurohaptics*. Citeseer, Birmingham, UK (2001) pp. 149–154.
11. J. Barbic and D. L James, "Six-dof haptic rendering of contact between geometrically complex reduced deformable models," *IEEE Trans. Haptics* **1**(1), 39–52 (2008).
12. M. A. Otaduy and M. C. Lin, "A modular haptic rendering algorithm for stable and transparent 6-dof manipulation," *IEEE Trans. Robot.* **22**(4), 751–762 (2006).
13. C. Duriez, F. Dubois, A. Kheddar and C. Andriot, "Realistic haptic rendering of interacting deformable objects in virtual environments," *IEEE Trans. Vis. Comput. Graph.* **12**(1), 36–47 (2006).
14. K. Huang and D. J. Lee, "Consensus-based peer-to-peer control architecture for multiuser haptic interaction over the internet," *IEEE Trans. Robot.* **29**(2), 417–431 (2013).
15. G. Sankaranarayanan and B. Hannaford, "Experimental internet haptic collaboration using virtual coupling schemes," *Proceedings of the IEEE Symps. on Haptic Interfaces for Virtual Environments & Teleoperator Systems*, Reno, NV, USA (2008) pp. 259–2008.
16. D. A. Lawrence, "Stability and transparency in bilateral teleoperation," *IEEE Trans. Robot. Autom.* **9**(5), 624–637 (1993).
17. J. E. Colgate and G. G. Schenkel, "Passivity of a class of sampled-data systems: Application to haptic interfaces," *J. Robot. Syst.* **14**(1), 37–47 (1997).
18. D. J. Lee, "Extension of Colgate's passivity condition for variable-rate haptics," *Proceedings of IEEE/RSJ International Conference on Intelligent Robots & Systems*, St. Louis, USA (2009) pp. 1761–2009.
19. J. M. Brown and J. E. Colgate, "Minimum mass for haptic display simulations," *Proceedings of the ASME International Mechanical Engineering Congress and Exhibition*, Anaheim, CA, USA (1998) pp. 249–1998.
20. D. J. Lee and K. Huang, "On passive non-iterative varying-step numerical integration of mechanical systems for haptic rendering," *Proceedings of ASME Dynamic Systems & Control Conference*, Ann Arbor, MI, USA (2008) pp. 1147–2008.
21. D. J. Lee and P. Y. Li, "Passive bilateral control and tool dynamics rendering for nonlinear mechanical teleoperators," *IEEE Trans. Robot.* **21**(5), 936–951 (2005).
22. D. J. Lee and P. Y. Li, "Passive decomposition of mechanical systems with coordination requirement," *IEEE Trans. Autom. Control* **58**(1), 230–235 (2013).
23. W. H. Chen, D. J. Ballance, P. J. Gawthrop and J. O'Reilly, "A nonlinear disturbance observer for robotic manipulators," *IEEE Trans. Indurstrial Electron.* **47**(4), 932–938 (2000).
24. A. Gupta and M. K. O'Malley, "Disturbance-observer-based force estimation for haptic feedback," *J. Dyn. Syst. Meas. Control* **133**(1), 014505 (2011).
25. J. J. E. Slotine and W. Li, *Applied Nonlinear Control*, vol. 199 (Prentice-Hall Englewood Cliffs, NJ, 1991).
26. M. Franken, S. Stramigioli, S. Misra, C. Secchi and A. Macchelli, "Bilateral telemanipulation with time delays: A two-layer approach combining passivity and transparency," *IEEE Trans. Robot.* **27**(4), 741–756 (2011).
27. D. J. Lee and K. Huang, "Passive-set-position-modulation framework for interactive robotic systems," *IEEE Trans. Robot.* **26**(2), 354–369 (2010).
28. D. J. Lee and M. W. Spong, "Passive bilateral teleoperation with constant time delay," *IEEE* **22**(2), 269–281 (2006).
29. E. Nuno, R. Ortega, N. E. Barabanov and L. Basanez, "A globally stable pd-controller for bilateral teleoperators," *IEEE Trans. Robot.* **24**(3), 753–758 (2008).

30. M. Kim and D. J. Lee, "Toward transparent virtual coupling for haptic interaction during contact tasks," *Proceedings of World Haptics Conference*, Daejeon, Korea (2013) pp. 163–2013.
31. O. Khatib, "A unified approach for motion and force control of robot manipulators: The operational space formulation," *IEEE J. Robot. Autom.* RA-**3**(1), 43–53 (1987).
32. M. W. Spong, S. Hutchinson and M. Vidyasaga, *Robot Modeling and Control* (John Wiley & Sons, Hoboken, NJ, 2006).
33. J. M. Brown and J. E. Colgate, "Passive implementation of multibody simulations for haptic display," *Proceedings of ASME International Mechanical Engineering Congress & Exposition*, Dallas, TX, USA (1997) pp. 85–1997.
34. R. M. Murray, Z. Li and S. S. Sastry, *A Mathematical Introduction to Robotic Manipulation* (CRC, Boca Ranton, FL, 1993).
35. R. W. Daniel and P. R. McAree, "Fundamental limits of performance for force reflecting teleoperation," *Int. J. Robot. Res.* **8**, 811–830 (1998).
36. S. P. Buerger and N. Hogan, "Complementary stability and loop shaping for improved human-robot interaction," *IEEE Trans. Robot.* **23**(2), 232–244 (2007).
37. T. Iwasaki, S. Hara and H. Yamauchi, "Dynamical system design from a control perspective: Finite frequency positive-realness approach," *IEEE Trans. Autom. Control* **48**(8), 1337–1354 (2003).

https://doi.org/10.1017/S0263574715000545 Published online by Cambridge University Press